

Mineralogical study of base metal tailings with various sulfide contents, oxidized in laboratory columns and field lysimeters

S. C. Shaw · L. A. Groat · J. L. Jambor · D. W. Blowes · C. J. Hanton-Fong
R. A. Stuparyk

Abstract Oxidation of a flotation-derived, low-sulfide tailings containing approximately 0.4 wt.% S was compared with simultaneously oxidized tailings containing 1.0 wt.% S and 2.5 wt.% S to assess their acid generating characteristics. Each tailings type was exposed to oxidation for three years in laboratory columns and in lysimeter pits in the field. In these tailings the sulfide mineral of principal concern with respect to acid generation is pyrrhotite (Fe_{1-x}S). In past studies the alteration of pyrrhotite has been characterized by initial replacement with marcasite (FeS_2) and ferric iron sulfates, which are followed by development of ferric oxyhydroxides such as goethite and lepidocrocite. Macroscopic characterization of the tailings shows varying and progressive degrees of oxidation correlative with the three different sulfur contents. As expected, the tailings with the lowest sulfur content are the least oxidized, and those with the highest sulfur content have reacted the most. The column tests, which represent accelerated reaction conditions relative to those for the lysimeter pits, show much higher degrees of oxidation, and a markedly more distinct boundary between the oxidized and unoxidized zones; as well, differences among the three tailings types are more pronounced.

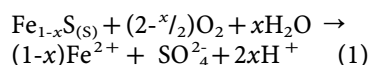
Key words Tailings · Sulfide minerals · Acid rock drainage

Introduction

Acid rock drainage (ARD), a term that has been used increasingly over the past quarter century, has become a problem for the mining industry as awareness and understanding of the consequences increase. ARD has commonly been defined as seepage, with a pH less than 5, originating from a tailings pile, a waste rock pile, or exposed sulfide-rich rock. It is not necessarily the acidity that is the direct problem; rather, it may produce deleterious effects arising from dissolved components that are solubilized by acidic solutions. ARD is typically enriched in soluble Fe, Mn, Ca, Mg, Al, SO_4 , and, at some locations, in heavy metals such as Pb, Cu, Zn, Ni, Co, As, and Cd. Acidic waters can cause discoloration and turbidity in receiving waters, but it is the loading of ions mobilized by the acid that can cause a decrease in aquatic flora and fauna, bioaccumulation of metals, and reduction in the quality of groundwater.

The primary cause of acid generation is the oxidation of sulfide minerals, predominantly pyrite and pyrrhotite. Many factors contribute to sulfide oxidation, including: (1) the pH of solutions in contact with the sulfide minerals; (2) the origin, chemistry, surface area and morphology of the minerals; (3) concentrations of oxygen and ferric iron in solution; (4) the temperature; (5) galvanic interactions of the sulfides with coexisting minerals; and (6) bacterial interactions. The oxidation rate can vary for different minerals, and for individual minerals, because of variations in their thermodynamic properties, the kinetics of the system, and the presence or absence of precipitated secondary minerals.

Pyrrhotite, which is the mineral of principal concern in the Inco Ltd. Copper Cliff tailings basin, oxidizes at rates 20–100 times faster than pyrite (Nicholson and Scharer 1994). The general formula of pyrrhotite is Fe_{1-x}S , where x can vary from 0.125 (Fe_7S_8) to 0.0 (FeS). The iron deficiency and consequent presence of Fe^{3+} in the structure are considered to contribute to the high reactivity rate of pyrrhotite (Elberling and others 1994; Pratt and others 1994a, 1994b; Nicholson 1994; Knipe and others 1995). The overall reaction in which oxygen is the primary oxidant is given by:



Received: 31 October 1997 · Accepted: 27 May 1997

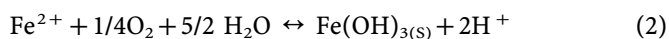
S. C. Shaw · L. A. Groat (✉)
Department of Earth and Ocean Sciences, University of British Columbia, Vancouver, British Columbia V6T 1Z4, Canada

J. L. Jambor
Leslie Investments Limited, Tsawwassen, British Columbia V4M 3L9, Canada

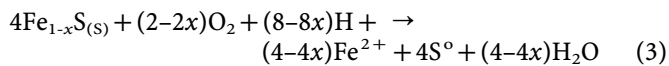
D. W. Blowes · C. J. Hanton-Fong
Waterloo Centre for Groundwater Research, University of Waterloo, Ontario N2L 3G1, Canada

R. A. Stuparyk
Process Technology-CC Mill, INCO Limited, Copper Cliff, Ontario P0M 1N0, Canada

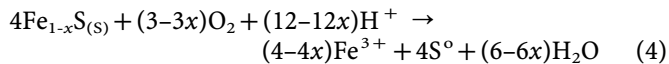
Oxidation and hydrolysis of the dissolved Fe^{2+} in Eq. 1 can result in the precipitation of ferric hydroxide and the creation of acid:



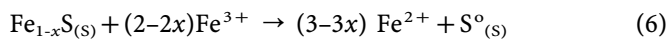
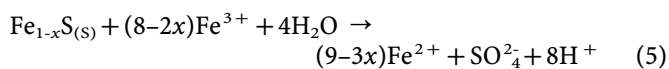
If the oxidation reactions do not go to completion, elemental sulfur can be produced via the reaction:



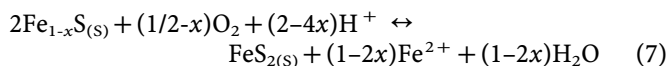
or



Ferric iron can also act as an oxidant of pyrrhotite. If the reaction goes to completion, sulfate ions can be produced as in Eq. 5. If the reaction does not go to completion, elemental sulfur may again be produced as an intermediate phase, Eq. 6:



Another common initial phase observed in the oxidative reaction of pyrrhotite is marcasite, FeS_2 . Its formation can be illustrated by the reaction:



The early developed phases, native sulfur and marcasite, are also metastable in the presence of oxygen in atmospheric concentrations and will eventually oxidize. Among the numerous preventative techniques being researched and/or employed by the mining industry to deal with ARD are underwater disposal (Robertson 1987), wetland treatment systems (Nolan and others 1987), neutralization by alkaline materials (Morin and Cherry 1986), inhibition of iron-oxidizing bacteria (Stichbury and others 1995), microencapsulation techniques (Hester and Associates 1984), and capping methods (Harries and Ritchie 1988). A variation of this last method is being examined by Inco Ltd., at their Copper Cliff tailings area. More than 10% of all tailings in Canada are located in the Copper Cliff tailings area, which makes it one of the largest reservoirs of potentially acid-generating tailings in North America. Deposition of the tailings began in the 1930s, and the tailings now occupy more than 2225 hectares. Upon closure, the estimated amount of tailings will be more than 720 million tonnes.

In the summer of 1993, Inco Ltd. began an extensive environmental assessment of a low-sulfur tailings product for use in impoundment dam construction and as a potential cover material upon closure. The assessment includes research by Inco Ltd., the Waterloo Centre for Groundwater Research, and the University of British Columbia to determine whether the low-sulfur tailings are suitable for use as a capping material. To make that decision, a study involving field lysimeter test pits and laboratory oxidation columns was set up to provide compari-

sons of the pathways and rates of oxidation of the low-sulfur tailings (0.4 wt.% S) versus those of a main tailings product (1.0 wt.% S) and a total tailings product (2.5 wt.% S). The low sulfur tailings are obtained by modification of the standard flotation treatment, and the resulting much smaller mass of sulfide-rich (about 12 wt.% S) tailings are discharged to a separate containment facility (Stuparyk and others 1995).

The production details of the low-sulfur tailings and the initial static and kinetic test work done prior to October 1995 were given by Stuparyk and others (1995). The results of their acid base accounting (ABA) tests, based on the British Columbia Acid Mine Drainage Task Force Guidelines (Steffen and others 1989), showed that the total tailings (2.5 wt.% S) are within the acid generating category. The main tailings (1.0 wt.% S) lie on the border between the acid generating category and the region of uncertainty, and the low-sulfur tailings (0.4 wt.% S), though producing a positive net neutralization potential (NNP) value, also fall into the region of uncertainty. Each of the three field lysimeters, constructed to hold approximately 180 tonnes of tailings, is approximately $15 \times 10 \times 2$ m and has a 1.1 mm thick polyethylene liner that isolates the contents from the surrounding groundwater. A drain beneath each lysimeter is used to tap the downflow originating from precipitation and snowmelt. The drains are composed of 10-cm ABS piping that is overlain by a drainage layer consisting of a 30-cm thickness of washed quartz sand, and the sand is overlain by a geotextile membrane. A monitoring program was set up by the Waterloo Centre for Groundwater Research to measure the pore-gas and pore-water compositions versus depth on a semiannual basis. The initial results were given by Blowes and others (1995).

The columns, designed to hold approximately 25 kg of unsaturated tailings, were constructed from PVC pipe approximately 15.3 cm in diameter, and were set up in triplicate for each of the tailings types. The tailings were placed on top of 20 cm of crushed quartz, which initially acted to hold the tailings in the columns. The columns are open at the top and are sealed at the bottom to mimic atmospheric conditions in the tailings basin. The tailings are irrigated with deionized water at a rate of 550 ml/week, or 25 mm/week (2.5 times more than the 87 cm of annual precipitation in the Sudbury region; Puro and others 1995). This volume is equivalent to the annual rainfall accelerated to occur in a 20-week period. The seepage from each column is collected in a sealed, anoxic collection flask. A U-tube attached to the base of the column provides the pathway for the seepage to collection flasks and prevents oxygenation of the base of the column. The pH, redox potential, specific conductance, total alkalinity, acidity, SO_4^{2-} concentration and major metal concentrations were analyzed weekly, and chemical characterization of the solid samples was done for each of the tailings types. The initial results were given in Stuparyk and others (1995).

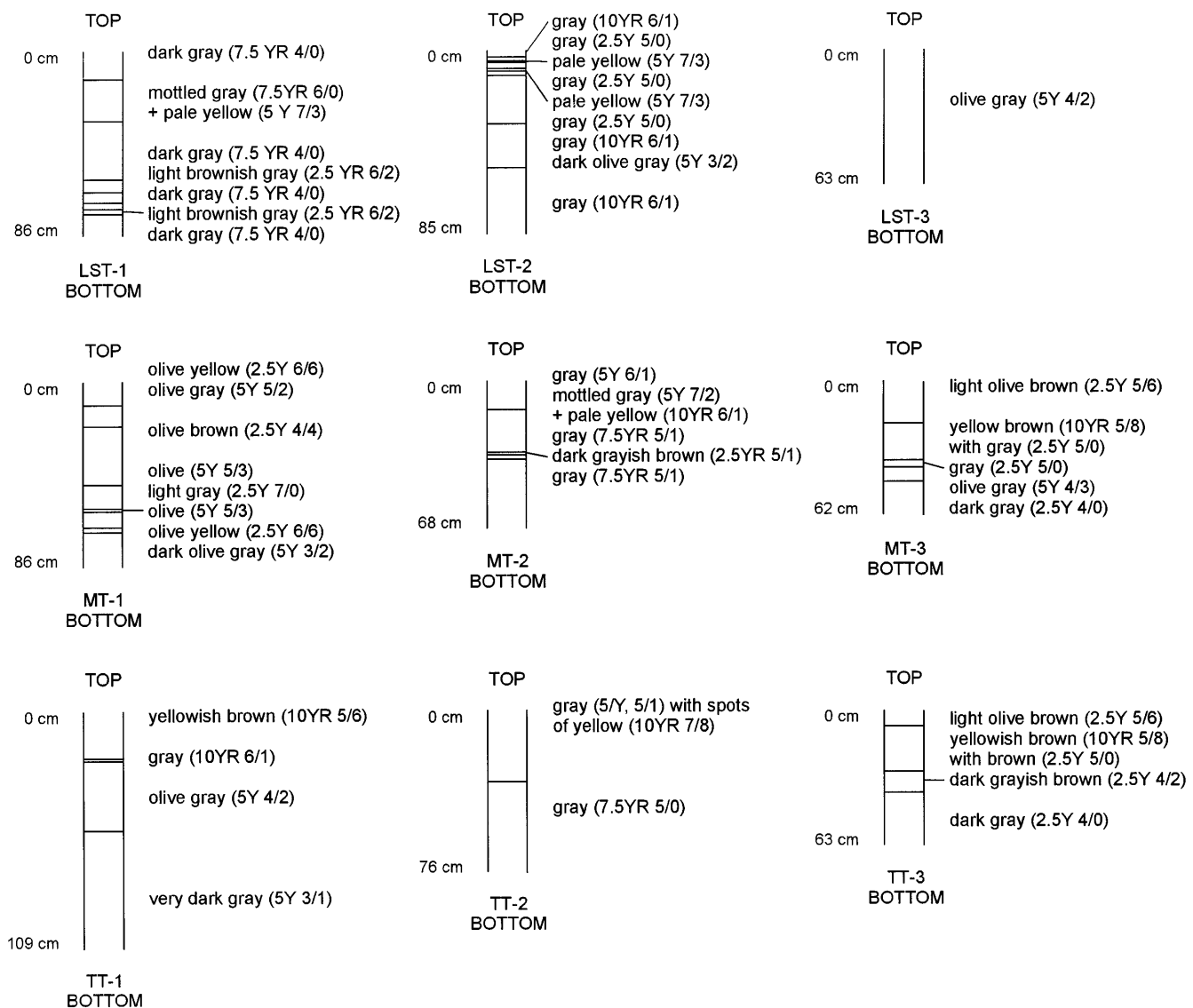


Fig. 1 Megascope color variation versus depth (LST low-sulfur tailings, MT main tailings, TT total tailings). The alphanumeric codes correspond to Munsell's soil color chart

Sampling and analytical procedures

Sampling for the mineralogical examination took place in October 1995, approximately 2.5 years after the installation of the field lysimeters. The lysimeters were cored vertically with 5-cm diameter aluminum tubes bottom-capped with iris cups to secure the tailings as the cores were extracted from the pits. Two cores were taken in each lysimeter, one where the surface of the tailings was dry and the other where the surface was wet. The core interval extended to the approximate depth of the lysimeters, ensuring that the liner was not punctured. Cored sites were within 1 m of piezometers previously placed

in the pits. The laboratory oxidation columns were cored using 2.5-cm diameter stainless steel pipes equipped with iris cups on one end. The tubes were driven vertically through the center of the columns to the depth of the quartz sand layer.

After sampling, the cores were frozen to prevent reactions between the tailings and core barrel, and to minimize any bacterially catalyzed reactions within the tailings. While frozen, the cores were split along their lengths; half was retained frozen as reference material, and the other half was thawed and dried at room temperature. Megascope characterization of the cores took place at this time, including grain size classification and color indexing of the tailings using Munsell's soil color chart. Subsamples of the tailings (approximately 90 in total) were taken at various depths throughout each core. Sampling was more closely spaced in the unsaturated zone than in the saturated zone of the cored tailings. These subsamples were then split; half was kept for x-ray diffraction analysis, and the other half was used for polished thin sections for optical and scanning electron microscop-

py. Preparation of the polished thin sections was done in kerosene so as to preserve any soluble phases present in the tailings.

Powder x-ray diffraction analyses were completed on dried tailings samples using a Siemens D5000 powder x-ray diffractometer with a graphite monochromator, $\text{CuK}\alpha$ radiation, a voltage of 40 kV, and a current of 30 mA. The samples were scanned from 3° to $60^\circ 2\theta$ in steps of 0.02° per 0.8 seconds.

A Nikon SMZ-1 OPTIPHOT2-POL stereoscopic microscope was used for the optical studies. Characterization included identification of the primary minerals and their alteration products, with emphasis on the alteration products and resulting textures. Potentially acid-generating minerals and acid-neutralizing minerals were closely examined for evidence of oxidation and dissolution. Specific grains were chosen for more meticulous examination using a Philips XL 30 scanning electron microscope equipped with a Princeton Gamma Tech IMIX energy dispersion spectroscopy (EDS)/image analysis system. The polished thin sections were carbon coated prior to analysis. Multielement x-ray maps were generated to more closely examine the secondary phases, many of which were mixtures of various fine-grained, poorly crystalline phases.

Results and discussion

Megascope characterization

The grain size of the tailings is predominantly that of sand (approximately 0.5 mm in diameter), with minor layers of silt (≤ 0.25 mm in diameter). Megascope characterization of the cores is shown in Fig. 1, which represents the color variations seen with depth. The cores from the unsaturated zone of the field lysimeters are gray in the low-sulfur tailings, whereas those from the total tailings (highest sulfur) are yellowish brown, and those from the main tailings (intermediate sulfur) fall between the two. The cores taken from areas in which the lysimeter surface was wet are consistently grayer in color than cores taken where the tailings were dry. The cores from the saturated zone of the lysimeters were nearly uniformly gray in all three types of tailings.

The oxidation columns exhibited a more distinct difference with respect to degree of oxidation between the low-sulfur tailings and the other two tailings types. The low-sulfur tailings column was an olive gray color throughout its depth, but the main tailings and total tailings columns varied from light olive brown at the surface to dark gray at the bottom, approximately in the same proportion in both columns.

Powder x-ray diffraction

X-ray diffractometer patterns for samples taken from the field lysimeters and the oxidation columns were used to identify the primary minerals, which are quartz, feldspar (plagioclase), mica (biotite), amphibole (hornblende-acti-

nolitic hornblende), chlorite, and pyroxene (both orthopyroxene and clinopyroxene).

Minerals that form within tailings after deposition are categorized as secondary (Jambor 1994). In the lysimeters, these minerals were determined by x-ray diffractometry to consist of gypsum, goethite, jarosite, and a vermiculite-type clay mineral. The gypsum was found in the main tailings lysimeter below 10 cm depth, and in both the main tailings and total tailings columns near surface and below 40 cm depth. The relative abundance of gypsum was greater in the near-surface samples, where the mineral was likely precipitated from solutions generated by sulfide oxidation; however, the gypsum seen at lower depths in the tailings is interpreted to have precipitated from mill waste waters that were codeposited with the tailings. Goethite and jarosite were detected in the total tailings column only in near-surface samples, and these minerals also are interpreted to have been derived from sulfide oxidation. A vermiculite-type mineral associated with the alteration of biotite occurs in near-surface samples from both the main tailings and total tailings columns.

Petrographic examination

The microscopic examination of the tailings confirmed the identification of the minerals listed above and identified apatite, pyrrhotite, magnetite, ilmenite, chalcopyrite, pentlandite, minor pyrite, and various secondary oxidation products which were below the detection limit of x-ray diffractometry. The main difference among the three tailings types with respect to primary mineralogy is in

Table 1
Sulfide alteration index for the lysimeter tailings

Numerical scale	Description of degree of sulfide alteration
10	Pyrrhotite and pentlandite completely obliterated, traces of pyrite and chalcopyrite may still be visible
9	Pyrrhotite is absent, but pentlandite with thick alteration rims may be present
8-7	Trace amounts of pyrrhotite may be seen as surviving cores in a pseudomorphic replacement; pentlandite still rimmed
6-4	Pyrrhotite grains have broad alteration rims (thinning from scale 6 to scale 4), commonly multiphase. Pentlandite grains may have thin rims (at scale 6) or show slightly altered edges (at scale 4)
4-2	Rims surrounding pyrrhotite thin as scale grades down to 2, and many grains appear unaltered. Pentlandite appears fresh
1-0	Very few grains of pyrrhotite are altered at an index of 1, usually along fractures or discontinuously at grain margins. At a scale of 0, all the grains are pristine

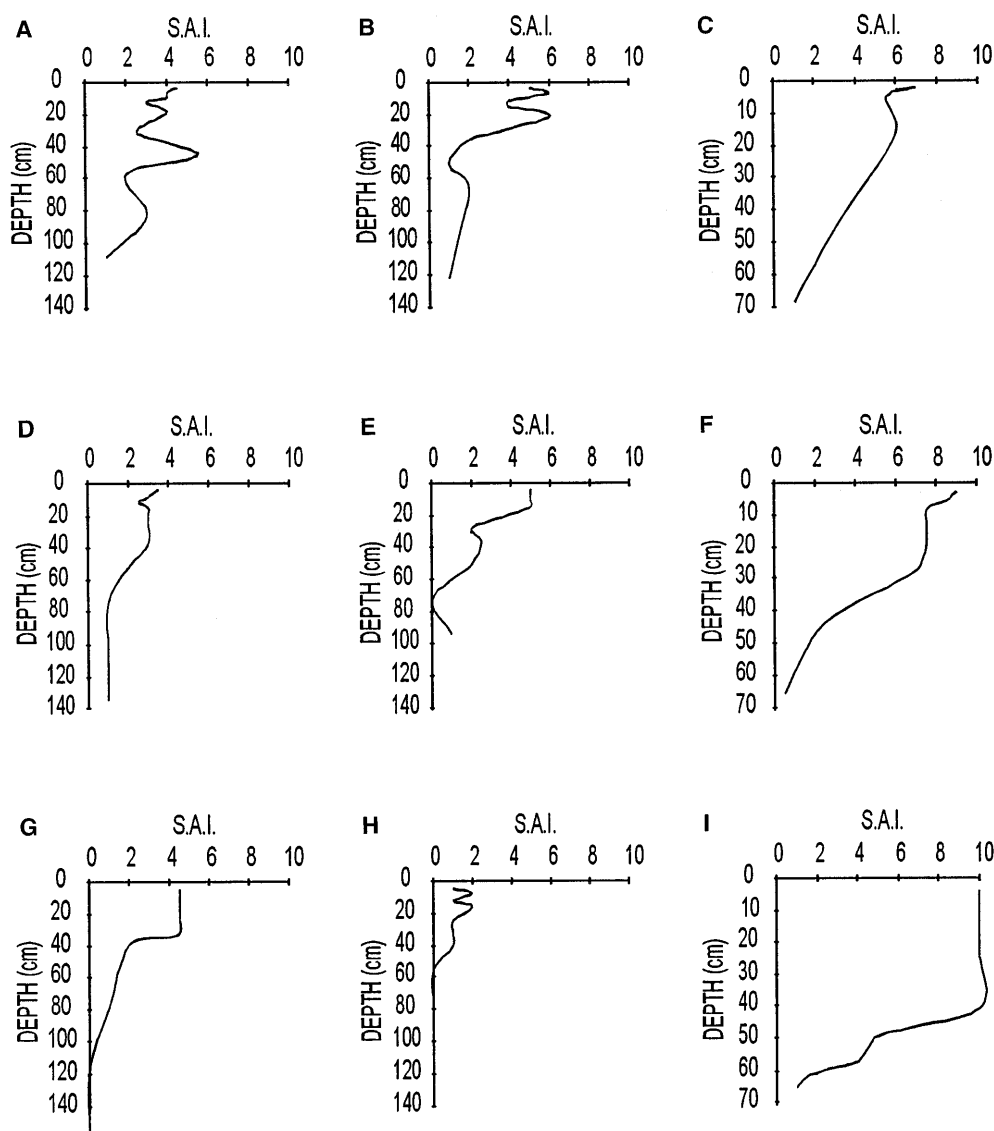


Fig. 2

Sulfide alteration index versus depth: A low-sulfur tailings lysimeter (surface of tailings wet); B low-sulfur tailings lysimeter (surface of tailings dry); C low-sulfur tailings oxidation column; D main tailings, lysimeter (surface of tailings wet); E main tailings, lysimeter (surface of tailings dry); F main tailings, oxidation column; G total tailings, lysimeter (surface of tailings wet); H total tailings, lysimeter (surface of tailings dry); I total tailings, oxidation column

their pyrrhotite content; the low-sulfur tailings contain approximately 1.5% pyrrhotite, the main tailings have approximately 2–3%, and the total tailings have 4–5% pyrrhotite in the unaltered samples. It is in this difference that the variation of acid-generating potential of the three tailings types lies. The oxidation of pyrrhotite is the primary cause of acid generation in the Copper Cliff tailings.

Oxidation of pyrrhotite in the tailings typically is manifested by various degrees of pseudomorphic replacement by secondary phases. This replacement initially occurs by penetration along fractures, partings, and around grain boundaries, advances to a stage in which only residual sulfides remain, and culminates in complete pseudomorphism.

The oxidation of pyrrhotite appears to have followed the same progression in all three tailings types, both in the lysimeters and the oxidation columns, the only difference having been in the degree of oxidation that had occurred prior to sampling. In order to draw comparisons among

the different tailings and the different experimental regimes, a sulfide alteration index was assigned to each sample and plotted against depth. The sulfide alteration index used was a modified version of that given by Blowes and Jambor (1990). It is based on a relativity scale ranging from 0 to 10. Table 1 outlines the characteristics used to assign a value to each sample. The sulfide alteration index was assigned to each sample on the basis of petrographic examination; the indices were plotted and the resulting profiles for the field lysimeter test pits and oxidation columns are given in Fig. 2.

Scanning electron microscopy

Scanning electron microscopy and multielement x-ray mapping techniques were used to investigate the fine-grained, heterogeneous phases resulting from the oxidation of pyrrhotite. Within the low-sulfur tailings field lysimeter, oxidation of pyrrhotite has progressed along its parting plane and rims as shown in Fig. 3. The multielement x-ray maps in this figure outline the chemistry of

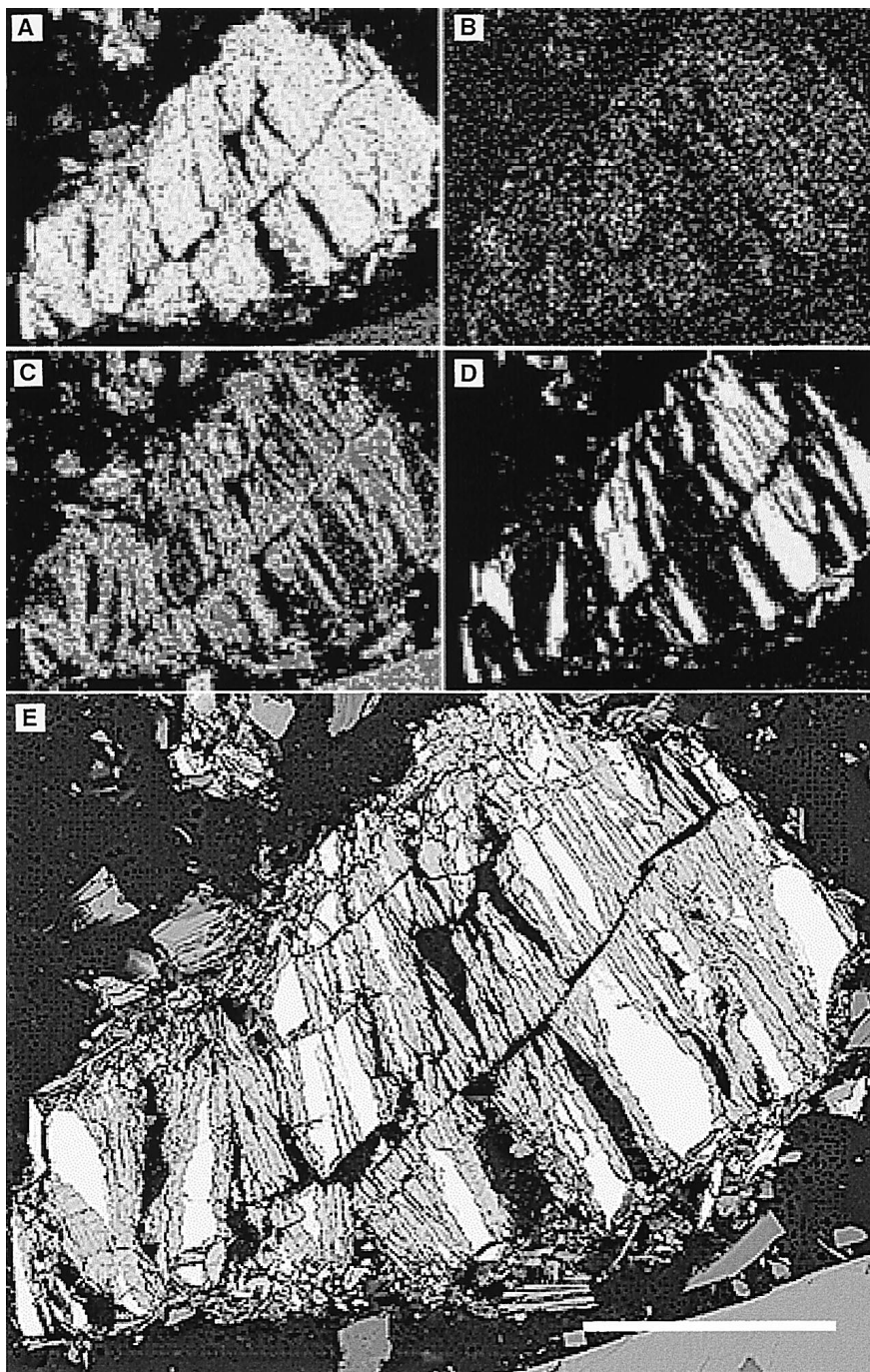


Fig. 3

Multielement x-ray maps and backscattered electron (BSE) image of altered pyrrhotite grain from low-sulfur tailings: A iron x-ray map; B nickel x-ray map; C oxygen x-ray map; D sulfur x-ray map; E BSE image of same grain. Scale equals 50 μ .

the alteration phase as well as the original grain, and it can be seen that this nickeliferous pyrrhotite is partly altered to a nickel-poor iron oxyhydroxide with residual sulfur detected sporadically in the alteration phase. The degree of alteration in the main tailings lysimeter pit can be illustrated by the grain depicted in Fig. 4. An iron oxyhydroxide phase and trace amounts of covellite replaced the pyrrhotite along the fractures and around the rim of the grain. The altered core of the grain, which is surrounded by pyrrhotite, has been replaced by a phase that has high Fe and S contents, but low optical reflectance, thus suggesting that the phase is an iron sulfate.

As oxidation proceeds beyond this stage, complete pseudomorphic replacement of pyrrhotite occurs in the total tailings (2.5 wt.% S) lysimeter (Fig. 5). Vestigial textures of the original pyrrhotite are present in the pseudomorphs as remnants of a weakly defined parting plane. The alteration phases include an iron oxyhydroxide rim and a core composed of both native sulfur and an iron sulfate. Similar textures and alteration products were seen in the oxidation columns. In all three columns, pyrrhotite replacement is more advanced than in the corresponding field lysimeters. The low-sulfur tailings in the oxidation

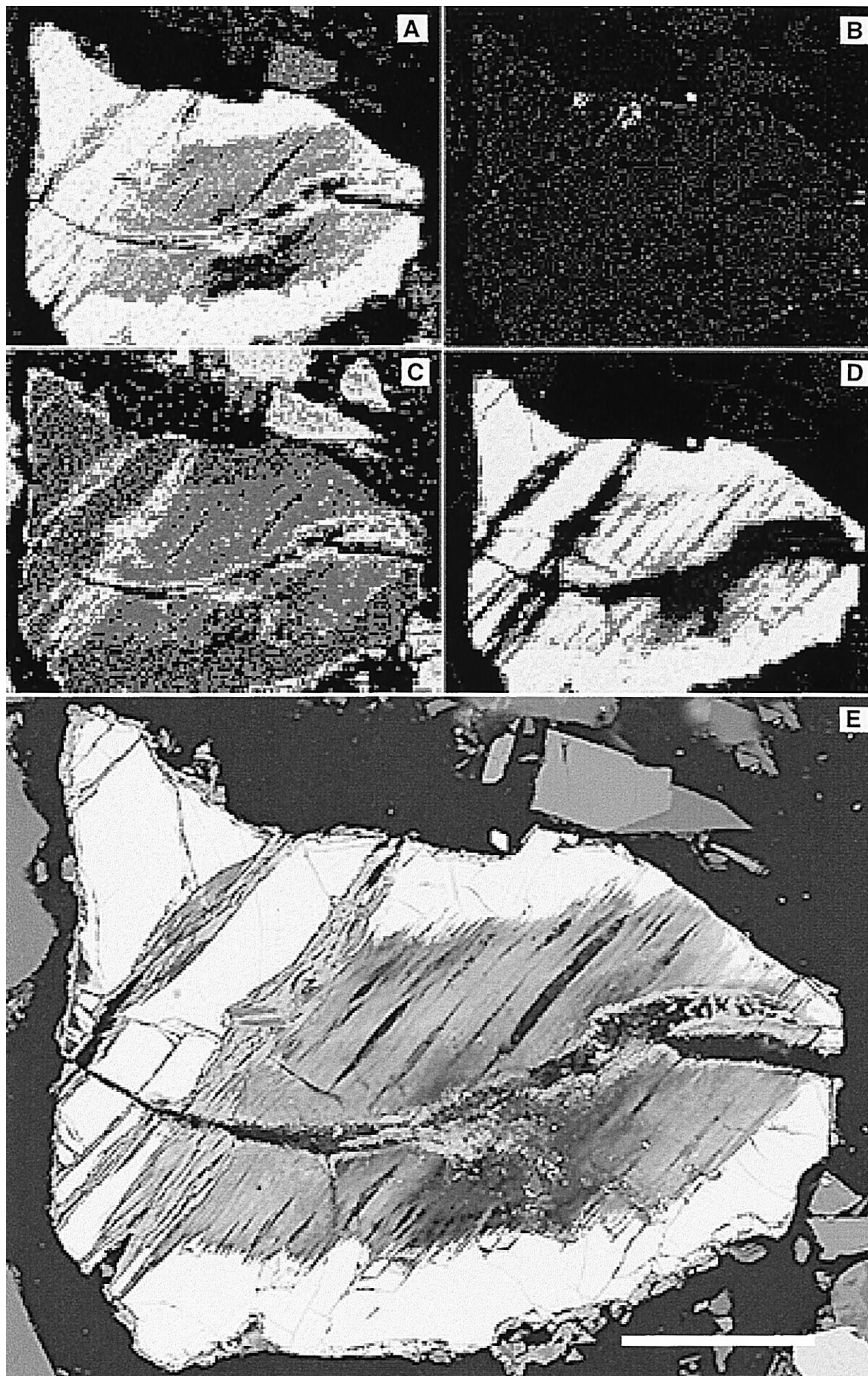


Fig. 4 Multielement x-ray maps and BSE image of altered pyrrhotite grain from the main tailings: A iron x-ray map; B copper x-ray map; C oxygen x-ray map; D sulfur x-ray map; E BSE image of same grain. Scale equals 50 μ .

column are more strongly oxidized than the counterpart in the field lysimeter, and are much less oxidized than both the main tailings (intermediate S) and total tailings (highest S) in the oxidation columns. The extent of oxidation in the main tailings and total tailings oxidation columns is also much greater than that seen in the field lysimeters. Oxidation of the main tailings and total tailings more closely approach one another in the columns than in the field lysimeters.

Conclusions

The low-sulfur tailings product (0.4 wt.% S) produced as a possible cover and construction material for the Copper Cliff tailings area was compared to a main tailings product (1.0 wt.% S) and a total tailings product (2.5 wt.% S) in an open-air field lysimeter test area as well as in laboratory oxidation columns. The degree of oxidation was greater in the oxidation columns than in the field lysimeter pits for all three tailings types, and in both experimental conditions the low-sulfur tailings were the least

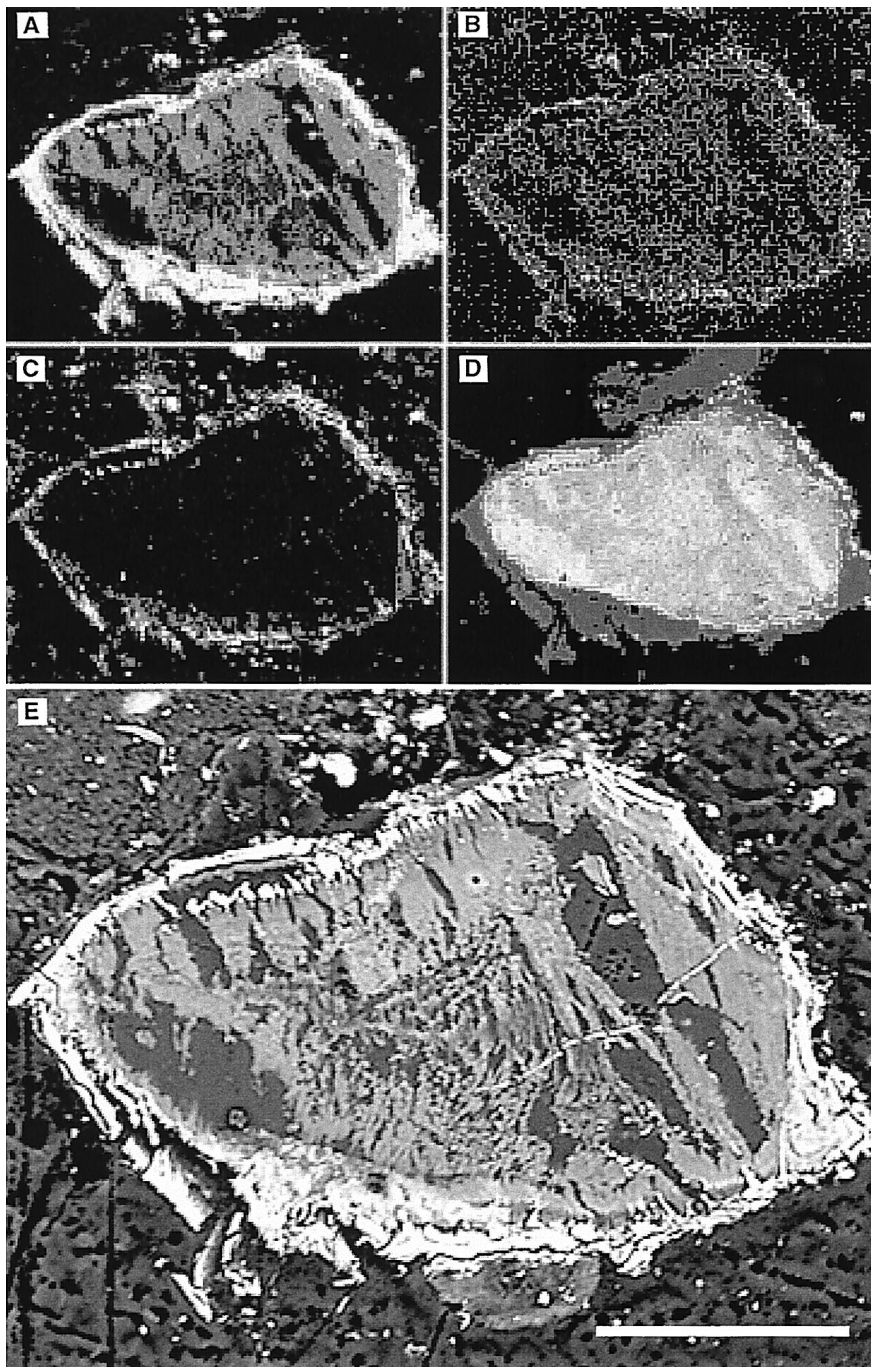


Fig. 5

Multielement x-ray maps and BSE image of altered pyrrhotite grain from the total tailings: **A** iron x-ray map; **B** nickel x-ray map; **C** oxygen x-ray map; **D** sulfur x-ray map; **E** BSE image of same grain. Scale equals 50 μ .

oxidized of the three tailings types. The main tailings (intermediate S) were markedly less oxidized than the total tailings (highest S) in the field lysimeter, and approach complete oxidation in the laboratory column. The total tailings material exhibited complete pseudomorphic replacement of pyrrhotite, which represents the highest degree of pyrrhotite oxidation in both the field lysimeter and the oxidation column. The secondary phases resulting from the oxidation of pyrrhotite, chalcopyrite, and pentlandite included goethite and possibly other iron oxyhydroxides, an iron sulfate, native sulfur, and covellite. The low-sulfur tailings will generate less acid because of the lower content of sulfide minerals. The decreased sul-

fide content has also slowed the rate of sulfide oxidation and attendant generation of acidity. These effects should have important benefits, in that the opportunity for potential neutralization by reaction with the silicate minerals is increased. Monitoring of the lysimeters is continuing in order to determine the extent to which the anticipated benefits are realized.

Acknowledgements The authors acknowledge the invaluable help of colleagues M. Raudsepp and J. McIntosh. Funding was provided by Inco Limited and by NSERC Research and IOR grants to LAG.

References

- BLOWES DW, JAMBOR JL (1990) The pore-water geochemistry and the mineralogy of the vadose zone of sulfide tailings, Waite Amulet, Quebec, Canada. *Appl Geochem* 5:327–346
- BLOWES DW, STUPARYK RA, HANTON-FONG CJ (1995) New approaches to the prevention of acid mine drainage. SSC File 0285Q.23440-4-1111, CANMET, Natural Resources Canada, Ottawa, Canada
- ELBERLING B, NICHOLSON RV, REARDON EJ, TIBBLE P (1994) Evaluation of sulphide oxidation rates: a laboratory study comparing oxygen fluxes and rates of oxidation product release. *Can Geotech J* 31:375–383
- HARRIES JR, RITCHIE AIM (1988) Rehabilitation measures at the Rum Jungle mine site. In: Salomons W, Förstner U (eds) *Environmental management of solid waste: dredged material and mine tailings*. Springer, Berlin Heidelberg New York, pp 131–151
- HESTER KD AND ASSOCIATES (1984) Practical considerations of pyrite oxidation control in uranium tailings. Contract 03Q83-00278, CANMET, Energy, Mines and Resources Canada, Ottawa, Canada
- JAMBOR JL (1994) Mineralogy of sulfide-rich tailings and their oxidation products. In: Jambor JL, Blowes DW (eds) *Environmental geochemistry of sulfide mine-wastes*. Mineralogical Association of Canada Short Course 22, Mineralogical Association of Canada, Nepean, Canada, pp 59–102
- KNIPE SW, MYCROFT JR, PRATT AR, NESBITT HW, BANCROFT GM (1995) X-ray photoelectron spectroscopic study of water adsorption on iron sulphide minerals. *Geochim Cosmochim Acta* 59:1079–1090
- MORIN KA, CHERRY JA (1986) Trace amounts of siderite near a uranium tailings impoundment at Elliot Lake, Ontario, and its implication in controlling contaminant migration in a sand aquifer. *Chem Geol* 56:117–134
- NICHOLSON RV (1994) Iron-sulfide oxidation mechanisms: laboratory studies. In: Jambor JL, Blowes DW (eds) *Environmental geochemistry of sulfide mine-wastes*. Mineralogical Association of Canada Short Course 22, Mineralogical Association of Canada, Nepean, Canada, pp 163–183
- NICHOLSON RV, SCHARER JM (1994) Laboratory studies of pyrrhotite oxidation kinetics. In: Alpers CN, Blowes DW (eds) *Environmental geochemistry of sulfide oxidation*. American Chemical Society, Symposium Series 550, American Chemical Society, Washington D.C., pp 14–30
- NOLAN, DAVIS AND ASSOCIATES (1987) Study of acid waste rock management at Canadian base metal mines. DSS File 23317-6-1738/01-SQ, CANMET, Energy, Mines and Resources Canada, Ottawa, Canada
- PRATT AR, MUIR IJ, NESBITT HW (1994a) X-ray photoelectron and Auger electron spectroscopic studies of pyrrhotite and mechanism of air oxidation. *Geochim Cosmochim Acta* 58:827–841
- PRATT AR, MUIR IJ, NESBITT HW (1994b) Generation of acids from mine waste: oxidative leaching of pyrrhotite in dilute H₂SO₄ solutions at pH 3.0. *Geochim Cosmochim Acta* 58:5147–5159
- PURO MJ, KIPKIE WB, KNAPP RA, McDONALD TJ, STUPARYK RA (1995) Inco Copper Cliff tailings area. In: Hynes TP, Blanchette MC (eds) *Proceedings of Sudbury '95 - Mining and the Environment*. CANMET, Natural Resources Canada, Ottawa, Canada, pp 181–191
- ROBERTSON AM (1987) Alternative acid mine drainage abatement measures. In: *Mine reclamation symposium: focus on acid mine drainage*. Proceedings of the British Columbia Mine Reclamation Conference. Province of British Columbia, Victoria, Canada
- STEFFEN, ROBERTSON AND KIRSTEN (BC) Inc. (1989) *British Columbia Acid Mine Drainage Task Force Report, Draft Technical Guide 1*. British Columbia Ministry of Energy, Mines and Petroleum Resources, Victoria, Canada, pp 6–12
- STICHBURY M, BÉCHARD G, LORTIE L, GOULD WD (1995) Use of inhibitors to prevent acid mine drainage. In: Hynes TP, Blanchette MC (eds) *Proceedings of Sudbury '95 - Mining and the Environment*. CANMET, Natural Resources Canada, Ottawa, Canada, pp 613–622
- STUPARYK RA, KIPKIE WB, KERR AN, BLOWES DW (1995) Production and evaluation of low sulphur tailings at INCO's Clabell mill. In: Hynes TP, Blanchette MC (eds) *Proceedings of Sudbury '95 - Mining and the Environment*. CANMET, Natural Resources Canada, Ottawa, Canada, pp 159–169